Fluorescence dynamics of lysosomal-related organelle flashing in the intestinal cells of *Caenorhabditis elegans*

Chieh-Hsiang Tan[#1], Keke Ding[#1,2], Mark G. Zhang[1], and Paul W. Sternberg[*1]

Division of Biology and Biological Engineering, California Institute of Technology, Pasadena, CA 91125, USA; [2]Present address: Innoland biosciences, Hangzhou, 310000, China

[#]: equal contribution

*: Corresponding author. E-mail: pws@caltech.edu

ORCID:

Chieh-Hsiang Tan: 0000-0002-5432-0160

Keke Ding: 0000-0002-5261-4843

Mark G. Zhang: 0000-0002-0802-300X

Paul W. Sternberg: 0000-0002-7699-0173

Abstract

The biological roles of the autofluorescent lysosome-related organelles ("gut granules") in the intestinal cells of many nematodes, including *Caenorhabditis elegan*s, have been shown to play an important role in metabolic and signaling processes, but they have not been fully characterized. We report here a previously undescribed phenomenon in which the autofluorescence of these granules increased and then decreased in a rapid and dynamic manner that may be associated with nutrient availability. We observed that two distinct types of fluorophores are likely present in the gut granules. One displays a "flashing" phenomenon, in which fluorescence decrease is preceded by a sharp increase in fluorescence intensity that expands into the surrounding area, while the other simply decreases in intensity. Gut granule flashing was observed in the different life stages of *C. elegans* and was also observed in *Steinernema hermaphroditum*, an evolutionarily distant nematode. We hypothesize that the "flashing" fluorophore is pH-sensitive, and the fluorescence intensity change results from the fluorophore being released from the lysosome-related organelles into the relatively higher pH environment of the cytosol. The visually spectacular dynamic fluorescence phenomenon we describe might provide a handle on the biochemistry and genetics of these lysosome-related organelles.

Introduction

The intestinal cells of the free-living soil nematode *Caenorhabditis elegans* contain a type of organelle known as gut granules, suggested to be the rhabditin granules observed in other nematodes in the order Rhabditida (Maupas 1900; Cobb 1914; Hedrick 1935; Chitwood and Chitwood 1950; Thomas and Quastler 1950; Laufer et al. 1980). The

birefringent and autofluorescent gut granules are robustly present in intestinal cells and intestinal precursor cells (Laufer et al. 1980; Hermann et al. 2005) and are so prominent that they have served as useful markers for the intestinal cell lineage in *C. elegans* development. Based on morphological, biochemical, and genetic evidence, these granules are characterized as lysosome-related organelles (Clokey and Jacobson 1986; Kostich et al. 2000; Hermann et al. 2005; Delevoye et al. 2019). While far from being fully characterized, previous studies found these organelles to be associated with metabolism and homeostasis processes such as the storage of fat, cholesterol, and heme (Schroeder et al. 2007; Lee et al. 2015; Sun et al. 2022) and the storage and sequestering of trace metals (Roh et al. 2012; Chun et al. 2017). Gut granules are also known to be involved in the biogenesis of small signaling molecules, such as ascarosides, and in the resistance to stress and pathogens (Le et al. 2020; Hajdu et al. 2023).

In this study, we found that some autofluorescent granules in the intestine of nematodes underwent a rapid and dynamic change in fluorescence intensity. The phenomenon depends on the worm ortholog of human Rab32/38, *glo-1* (Gut granule LOss) (Hermann et al. 2005; Morris et al. 2018), which has been shown to be required for gut granule biogenesis, suggesting that gut granules were the source of the autofluorescent flashing signals. High-resolution confocal imaging of *ex-vivo*, partially exposed *C. elegans* intestines found the spatial-temporal patterns of the fluorescence intensity changes in green and red to be different. Thus, we reason that at least two distinct types of fluorophores or fluorophore transitions are present in the gut granules. Green fluorescence intensities in the granules sharply increased, rapidly extended, or diffused to the surrounding areas and then dissipated, a phenomenon that we describe

as “gut granule flashing.” No similar rapid increase in red fluorescence intensities was observed prior to their simultaneous dissipation with the green. Gut granule flashing was found in multiple life stages of *C. elegans* as well as in the first juvenile (J1) larval stage of *Steinernema hermaphroditum*, an evolutionarily distant nematode. This intriguing phenomenon provides an assay with which to explore the functions and mechanisms of lysosome-related organelles, though the fluorophores responsible and the underlying biochemical processes remain unknown.

Results

Autofluorescent lysosome-related organelles in the intestine of *C. elegans* displayed dynamic changes in fluorescent intensities

We observed that the autofluorescent granules in the intestine of *C. elegans* spontaneously underwent dynamic changes in fluorescence intensity (Figure 1; Video S1, S2). The phenomena can be summarized as a sharp increase in the fluorescence intensity in the granules followed by a quick dissipation and “diffusion” into the surrounding area (Figure 1). We suspected that the phenomena were induced by the blue light used for excitation since it only occurs some time after the start of imaging process (Video S1,2). We observed this in at least two different stages during worm development: fourth stage (L4) larvae (19 of 20 worms) (Figure 1F-H; Video S2) and dauer stage larvae (15 of 20 worms) (Figure 1 A-E; Video S1).

We reasoned that these autofluorescent granules we observed are lysosome-related organelles known as gut granules (Laufer et al. 1980). To confirm this, we examined

glo-1(lf) worms deficient in gut granule biogenesis and observed neither these granules nor the flashing phenomena in the *glo-1(lf)* worms (L4, 0 of 11 worms) (Hermann et al. 2005), suggesting that the flashing granules are gut granules.

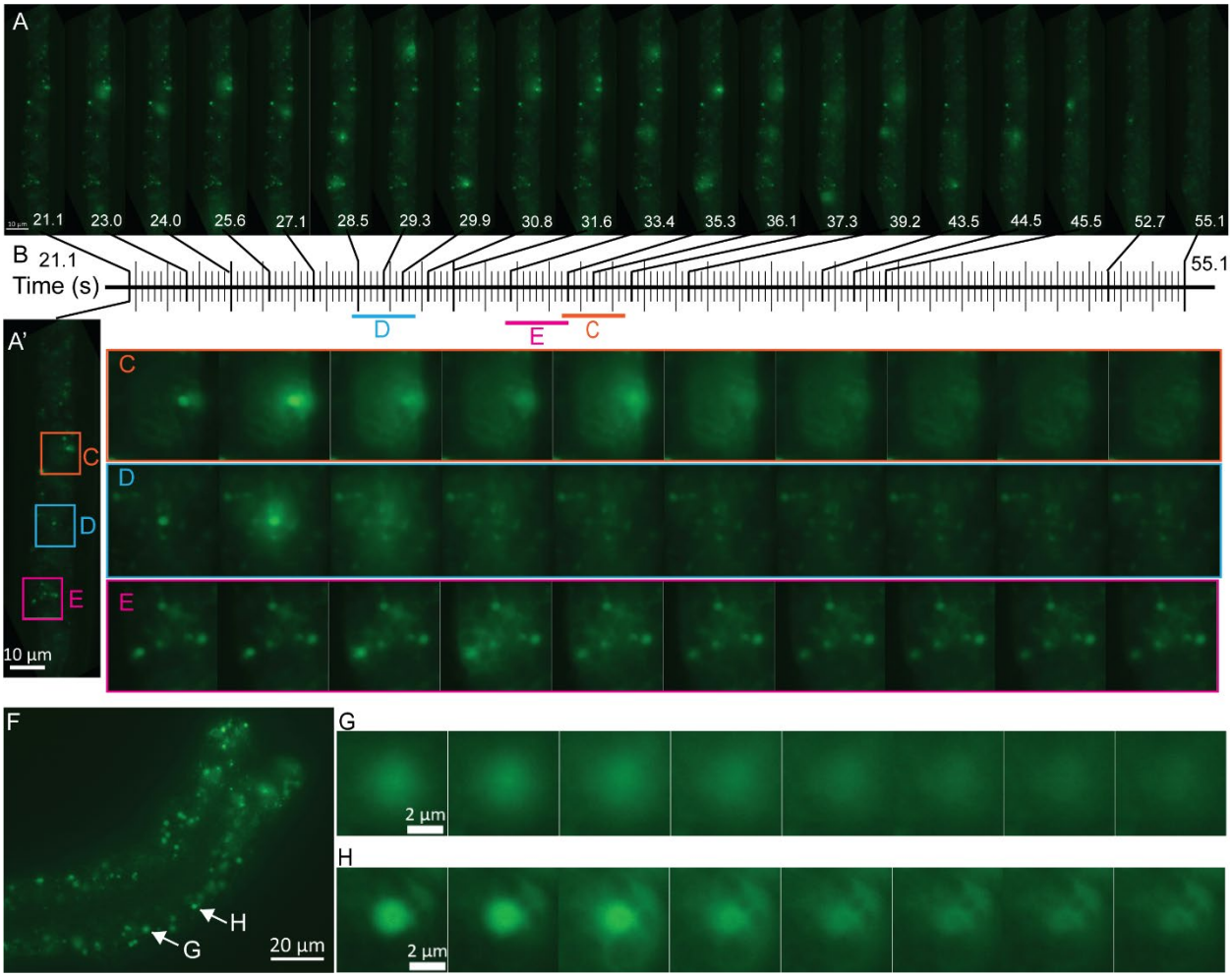

Figure 1 Autofluorescent granules in intestinal cells displayed dynamic changes in fluorescence intensities. (A-E) Dynamic fluorescence intensities change in intestinal granules of a dauer stage larva. (A) Fluorescence images (eGFP channel) of the intestine of a dauer stage larva of wild-type (N2) *C. elegans* at different time points during the analysis. Values represented are seconds and start (from 0) with the initiation of live imaging. The complete series of images are presented in Video S1. (A') An enlarged image of A at time 0, with sections represented in C-E indicated with boxes. Due to the movement of the animal, the positions of the granules were not exactly the same as in C-E. (B) A timeline positioning the images of A to E. Each vertical line represents an individual time point with an image taken. The images were acquired at a rate of ~5 frames

per second. (C-E) Enlargement of sections of the intestine shown in A, focusing on individual granules at the time of rapid intensities changes over periods of ~1.8 seconds. In each case, the dissipation of the granules' autofluorescence was preceded by an increase in intensity (2nd panel in C and D, 3rd in E) and then a "diffusing" cloud that increased the fluorescent intensities of the surrounding areas. In (C), fluorescence intensity changes in the 5th panel may be due to a second granule undergoing the process in a different focal plane. In (E), the granule can still be clearly observed after the event, albeit with decreased fluorescence intensities. (F-H) Fluorescent dynamic in intestinal granules of an L4 stage larva. (F) Fluorescent images (eGFP channel) of the intestine of an L4 stage larva of wild-type (N2) *C. elegans*. (G, H) Enlargement of sections of the intestine shown in F, focusing on individual granules at the time of the dynamic changes over periods of about 1.1 seconds. The complete series of images can be found in Video S2. Scale bar: (A, A'): 10μm; (F): 20μm; (G, H): 2μm.

Two types of fluorophores are likely present in the gut granules with distinct fluorescent dynamics

To investigate the dynamic of gut granule flashing, we extruded the intestines of L4 stage hermaphrodites by cutting the animal open posteriorly near the anus (Figure 2) and imaged the intestine using scanning confocal microscopy. Under this *ex-vivo* experimental setting, we were able to observe and characterize the fluorescence dynamics with increased resolution. However, in contrast to the *in-vivo* setting, we found gut granule flashing to be rare under this condition. Since the primary function of the intestine is food digestion, we reasoned that autofluorescent granules flashing could be associated with nutrient uptake. In *C. elegans*, food availability significantly influences the rhythmic defecation cycle (Thomas 1990), which is controlled by calcium oscillations in the intestinal cells (Dal Santo et al. 1999). To test whether gut granule flashing are associated with food availability, we provided food (*Escherichia coli* OP50) to the experimental animal on the microscopic slides (Figure 2). We found that in worms with a significant amount of food near the head region, the occurrence of the gut granule flashing

increased dramatically (Figure 3A-D; Video S3). All 7 recordings of worms provided with food displayed the phenomena (Figure 3C, D, H), while only 1 of 7 without food did, and at a low frequency (Figure 3A, B, H). We note that even in the “no food” group a trace amount of food is carried over during sample preparation, which may explain the one worm that exhibited the effect at a reduced level. It is unclear why the autofluorescent granules’ flashing phenomena in the *ex-vivo* setting are strongly correlated with food availability, but it may imply that gut granule flashing could be a part of or a consequence of a metabolic or signaling process in food intake. A possible explanation for the difference in food dependency in the *in-vivo* and *ex-vivo* settings is that only in the *ex-vivo* setting with no provision of food were the intestinal cells removed from the usual content of the intestinal lumen. In subsequent experiments in which we examined gut granule flashing in *ex-vivo* intestines, we provided food to increase the frequency of flashing.

To further test whether these flashing autofluorescent granules are gut granules, we analyzed the *ex-vivo* intestines of *glo-1(*lf*)* mutant animals. *glo-1(*lf*)* animals displayed a large reduction in the number of autofluorescent granules in the intestine, similar to what was described by Hermann et al. (2005), and also completely eliminated the granules’ flashing phenomena (Figure 3E, F, H). None of the seven *glo-1(*lf*)* animals displayed food-induced flashes of fluorescence as seen in all seven wild-type animals (Figure 3H), suggesting that the flashing autofluorescent granules are gut granules.

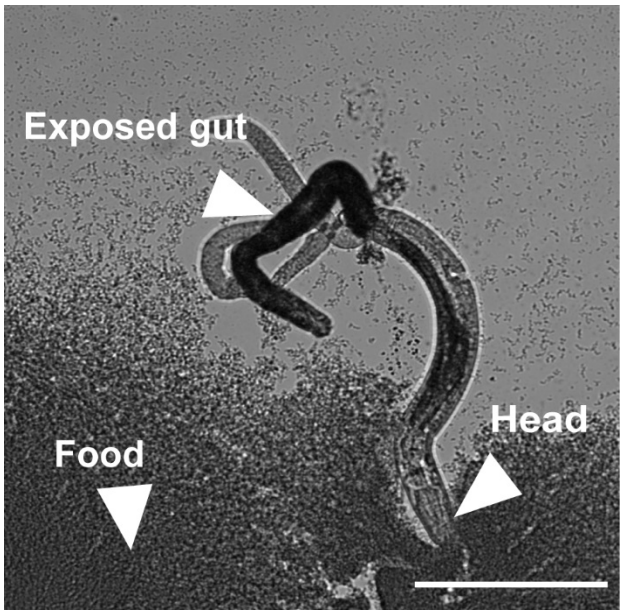

Figure 2 An example of the *ex-vivo* experimental preparation. L4 stage nematodes were carefully incised near the anus to expose the gut. In the “with food” conditions, nematodes were positioned to embed their heads in food. Scale bar: 200 μm.

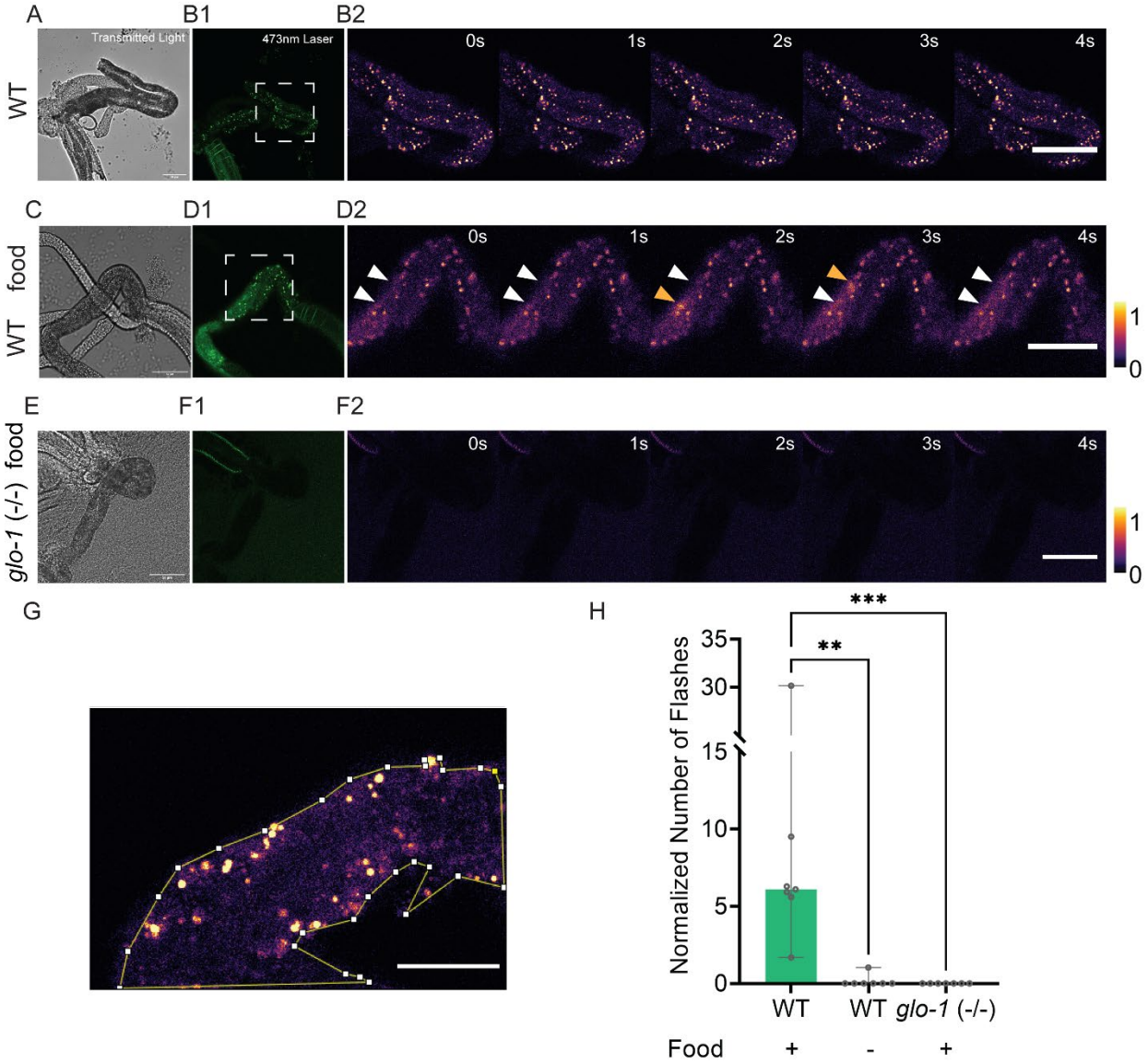

Figure 3 Gut granule flashing is correlated with food availability in the *ex-vivo* experimental setting. The field of view was illuminated and recorded with transmitted light (A, C, E), epifluorescence (B1, D1, F1), and 473nm laser illumination (B2, D2, F2). In (B2, D2, F2) 5-second clips of time-series with 473nm laser illumination were pseudo-colored and shown. (A-B) In wild-type worms not provided with food on the slide, the phenomena were rarely observed. (C-D) In wild-type worms provided with food on the slide, the occurrences of phenomena increased dramatically. Orange arrowheads in (D2) indicate the onset of gut granule flashing events. White arrowheads indicate the positions of those events before and after onset of the flash. (E-F) No gut granule fluorescence and no events were detected in *glo-1(lf)* worms even in the presence of food. (G-H) Gut granule flashing events were manually identified and analyzed. To normalize the number of events for comparison, the counts for each sample were temporally averaged in the area of exposed intestine within the field of view as shown in (G) (details in Materials and

Methods). (H) Normalized data from all conditions were plotted (N=6-7), and each group was compared with the wild-type (WT) + food group (**P<0.01, ***P<0.001, Mann-Whitney U test). Vertical bar indicates data range. Scale bar: (A-F): 50 μm; (G): 20 μm.

Analyzing wild-type worms under the *ex-vivo* setting provided with food, we observed that the green fluorescence, illuminated with the 473nm laser of the confocal microscope, rises sharply and significantly (Figure 4A-C; Video S3). The intensity increase is not only limited to the original “core” area (the granule proper, as identified by the high level of fluorescence prior to the event) but also to the surrounding areas (which we refer to as the “cloud,” details of how the area is identified are in Methods; Figure 4D). The fluorescence intensity in both the “core” and the “cloud” subsequently dropped off, with the intensity at the “core” decreasing to a level lower than that of the initial level, and the intensity in “clouds” recovered to the baseline (Figure 4D). On the other hand, when illuminated with the 561nm laser, the emitted red fluorescent lacked the initial sharp increase observed in green fluorescence but fell concurrently (Figure 4E). We estimated that the rapid changes in fluorescence intensity occur in under 10 seconds. The difference in the length of the event in the *in-vivo* and *ex-vivo* settings could be due to the difference in imaging. The differences observed in the dynamics of green and red fluorescence intensities suggest that they likely represent two distinct types of fluorophores. It is also possible, however, that they represent a single fluorophore with two distinct transitions. For simplicity, we will discuss in terms of two fluorophores.

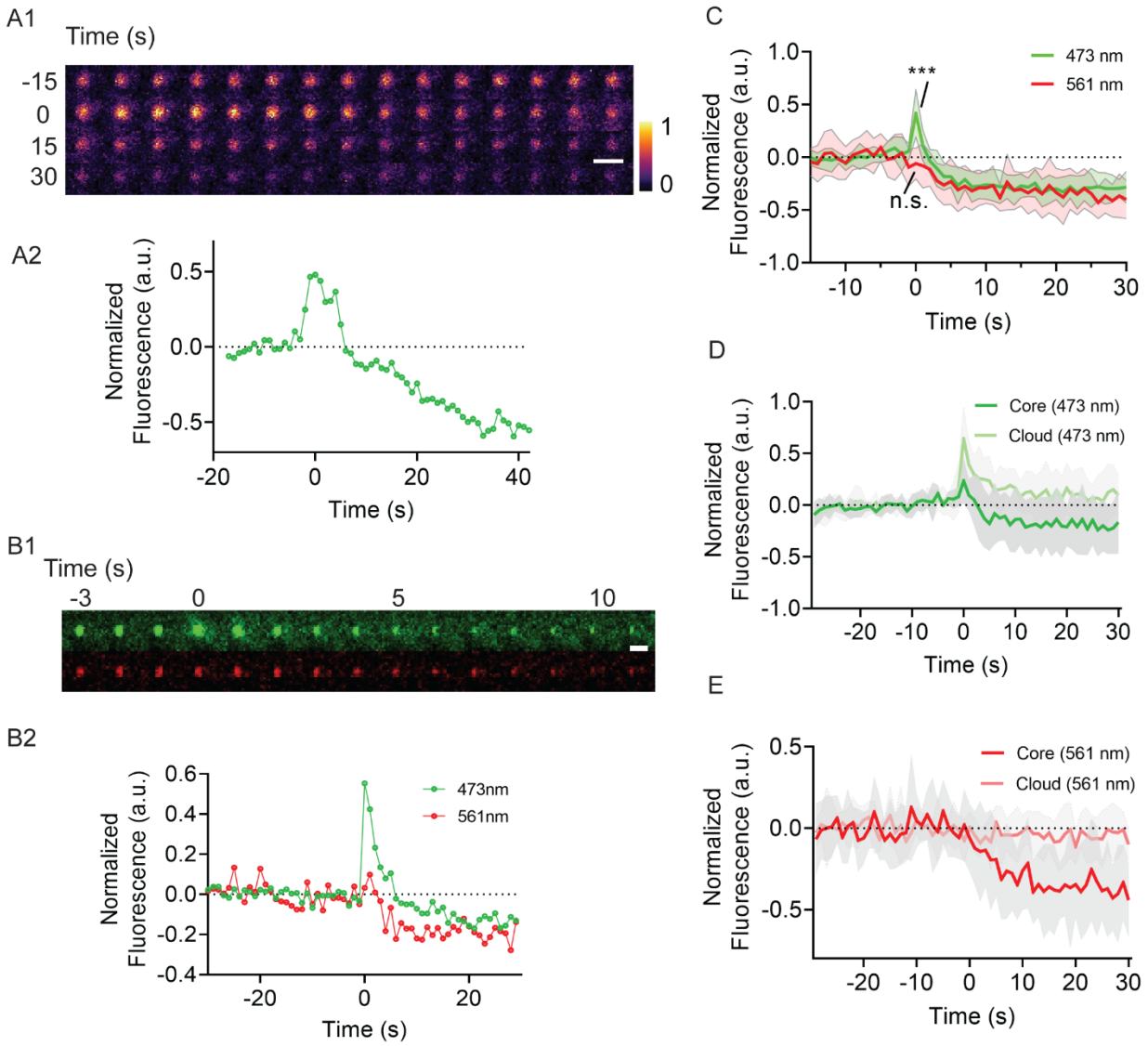

Figure 4 The dynamics of gut granule flashing. (A) The green fluorescence in the granule increases and falls sharply. Representative example of changes in green fluorescence during gut granule flashing. (A1) A 1-minute pseudo-color time series of a gut granule flashing event. Imaging rate: 1Hz. The time axis is zeroed at the onset of changes in fluorescence (see Methods). (A2) Normalized green fluorescence intensity plot of the same granule shown in (A1). (B-C) The green fluorescence in the granule increases and falls sharply, while the red lacks the initial sharp increase. (B) A representative example of two-color time-lapse imaging (B1) and normalized quantifications (B2). In A2 and B2, the fluorescence intensities of each granule are normalized by the baseline fluorescence calculated as the mean of fluorescence in the ROIs prior to the changes in fluorescence. (C) The average fluorescence intensity of all recorded flashing events in one sample. The green fluorescence shows a distinct peak after time 0, while the red fluorescence does not. (D-E) Gut granule flashes. Two-color imaging of all recorded gut granule flashing

events in a representative sample. The normalized fluorescence of each data point at time 0 in the green channel are compared to baseline (Normalized Fluorescence=0) and show statistically significant difference (***), while parallel comparison between red channel data point vs. baseline does not show significant difference (n.s.). (D-E) The granular area ("core"), as well as the surrounding ring area that presents diffusion of fluorescence ("cloud"), were measured separately in both 473nm (D) and 561nm (E) illumination. (D). The intensity increase in green fluorescence is not only limited to the original "core" area but also to the surrounding "cloud." (E) No intensity increase was observed with the red fluorescence, neither in the "core" nor the "." Raw images for analysis were identical to (C), except a longer pre-onset timeframe was selected for normalization. In (C-E), pooled values are presented as mean ± s.d (N=11 in D, N=8 in D and E). The time axis is zeroed at the onset of changes in fluorescence. Scale bar: 5 μm.

Gut granules do not play a significant role in the worms' avoidance of blue light

Since gut granule flashing may be associated with exposure to ~470 nm blue light, it is possible that this phenomenon is involved in the behavioral responses to blue light, namely negative phototaxis and feeding cessation (Ward et al. 2008; Edwards et al. 2008; Bhatla and Horvitz 2015). We found that exposure of worms to blue light increases the locomotion of *glo-1* mutant worms that are defective in gut granule biogenesis to a similar extent as wild-type worms (Figure 5). These results suggest that gut granules are not involved in the worms' light avoidance behavior.

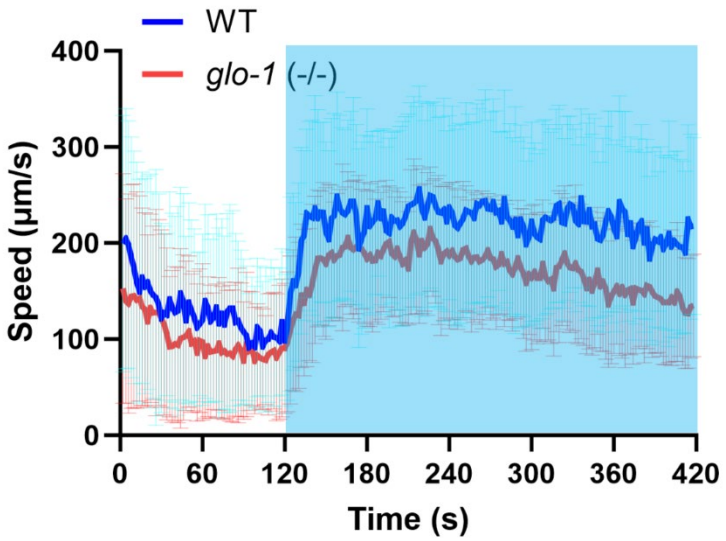

Figure 5 Gut granules do not play a significant role in the worms' avoidance of blue light. Both WT and *glo-1(zu391 lf)* worms respond to blue light applied between 120-420s (blue shade) by increased locomotion. Values are mean ± s.d (WT: n=57; *glo-1(zu391)*: n=52). *glo-1(zu391*lf*)* worms move slower with or without stimulus, which may partially be the result of having a smaller body size (Figure S1).

Gut granule flashing is conserved in nematodes

As similar granules are known to be common in Rhabditida nematodes (Maupas 1900; Cobb 1914; Hedrick 1935; Chitwood and Chitwood 1950; Thomas and Quastler 1950). We examined *Steinernema hermaphroditum*, one of the nematodes adopted for laboratory culture and genetic analysis most evolutionarily distant from *C. elegans* (Cao et al. 2022), to see whether it possessed similarly dynamic fluorescence in its gut granules.

The intestinal cells of *S. hermaphroditum* also contain autofluorescent granules (Figure 6A). While we did not observe gut granule flashing in *S. hermaphroditum* animals corresponding to the L4 and dauer larval stages of *C. elegans*, we did observe it in 9 of 10 first-stage J1 larvae (corresponding to the L1 larval stage in *C. elegans*) larvae (Figure

6). Thus, the underlying physiological conditions and the biochemical components that are responsible for gut granule flashing are likely to be shared among nematodes.

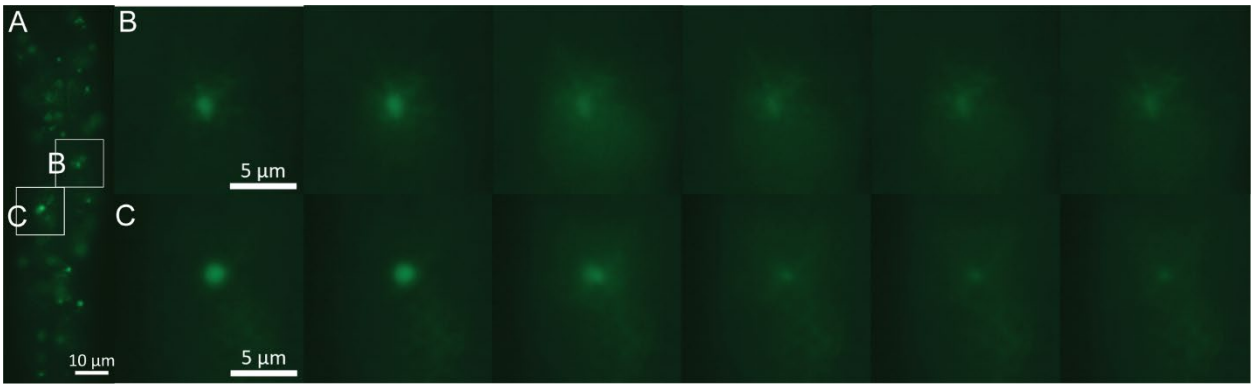

Figure 6 The flashing phenomena of autofluorescent granules in intestinal cells are shared among nematodes. (A) Epifluorescence images (eGFP channel) of the intestine of a J1 stage larva of wild-type *S. hermaphroditum*. Like those of *C. elegans*, the intestinal cells contain autofluorescent granules. Scale bar: 10µm. (B, C) Enlargement of sections of the intestine shown in A, focusing on individual granules at the time of the dynamic changes over periods of ~1 seconds. Scale bar: 5µm. The complete series of images can be found in Video S4.

Discussion

C. elegans have long been known to be autofluorescent (Babu 1974), with most of the autofluorescence coming from the gut granules (Clokey and Jacobson 1986). Particular interest has been paid to the increasing level of autofluorescence as the worms age or become stressed (Klass 1977; Davis et al. 1982; Clokey and Jacobson 1986; Forge and Macguidwin 1989; Pincus et al. 2016; Hajdu et al. 2023). However, the fluorophores responsible for gut granule autofluorescence remain largely undefined. One of the fluorophores emitting blue fluorescence has been identified as anthranilic acid (Babu 1974; Coburn et al. 2013), and changes in the blue fluorescence near the death of the

animals (death fluorescence, or DF) have been described (Coburn et al. 2013; Pincus et al. 2016). Both green and red fluorescence also increase with age, and the green fluorescence intensifies near the death of the animals (Coburn et al. 2013; Pincus et al. 2016). It is important to note that these fluorescence changes are distinct from the gut granule flashing phenomenon that we are describing in this research, both spatially and temporally.

In *C. elegans*, gut granules have been shown to have both metabolic and signaling functions. These lysosome-related organelles are a site for fat, cholesterol, and heme storage (Schroeder et al. 2007; Lee et al. 2015; Sun et al. 2022) as well as a storage and sequestering site for micronutrient metals (Roh et al. 2012; Chun et al. 2017). Gut granules are also the site of biosynthesis for signaling molecules such as ascarosides (Le et al. 2020). Recently, they have also been suggested to be involved in the responses to other forms of stress and in the resistance to pathogens (Hajdu et al. 2023). Other than being static sites of storage and metabolic processes, gut granules have been shown to undergo structural and morphological changes responding to changes in dietary conditions. In response to high dietary zinc, gut granules are remodeled from round spheres to bilobed granules with asymmetrical distribution of both internal content and membrane proteins (Roh et al. 2012). The mechanism of such a structural rearrangement remains largely uncharacterized.

In an attempt to develop the intestine of *C. elegans* as a model to study vesicle release using genetically encoded fluorescent markers, we discovered a novel food-dependent phenomenon of dynamic autofluorescence in intestinal lysosome-related organelles. When observed with the green fluorescence channel, these autofluorescent granules of

the nematode intestine underwent a rapid and dynamic change in intensity, a phenomenon we describe as “gut granule flashing.” Observable changes begin with a sharp increase in fluorescence intensity and end with rapid dissipation and diffusion. Further analysis suggests that two distinctive fluorophores or fluorophore transitions exist in the gut granules, with only one of them having the “flashing” characteristic.

Mechanistically, this could be either explained by the breakdown of the granule and the release of one or more of its constituents (Model 1. Figure 7A); or the release of some of the granule constituents by granules that remain intact (Model 2. Figure 7B). In both models, changes in the green fluorescence intensity may be explained by the green fluorophore responding to differences between the lysosome-related organelles and the cytoplasm. The lumens of the lysosome-related organelles are more acidic than the cytoplasm (Clokey and Jacobson 1986; Kostich et al. 2000; Hermann et al. 2005); If the green fluorophores are pH-sensitive, with fluorescence intensity positively correlated with pH, the green fluorophore would increase in fluorescence upon exiting the granules. On the other hand, the changes in red fluorescence intensity may be explained by the red fluorophore being pH-neutral. The subsequent dissipation and diffusion can also be reasonably explained as the diffusion of both of these molecules. We think Model 1 may be more likely (Figure 7A), partly because there is some similarity between our observation and that of Luke et al. (2007), in which fluorescently labeled gut granules disruption in osmotic sensitive mutants under hypotonic shock were shown. We do not exclude Model 2, however, as we noticed that it is not uncommon for residues of the autofluorescence to remain after the flashing event for individual granules (Figure 1E), and in the *ex-vivo* confocal recorded experiments, we have also observed multiple

flashing events in some of the granules, both of which argued against the disruption of the granules and support substance release by intact granules as described in Model 2 (Figure 7B). It is also possible that the event described in both models occurs but in different granules.

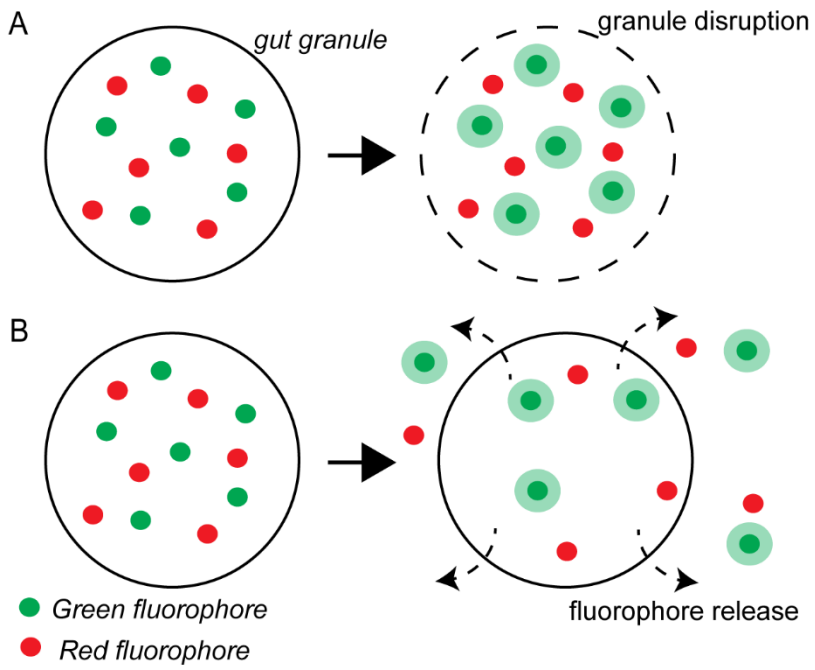

Figure 7 Models for the gut granule flashing. In both models, the green fluorophores are pH-sensitive, with fluorescence intensity positively correlated with pH. On the other hand, the red fluorophores are likely pH-neutral. A) In the first model, the fluorescence dynamic is explained by the breakdown of the granule and the release of its constituents. The fluorescence of the green fluorophores increases after breakdown due to the higher pH environment in which the fluorophores now reside. B) In the second model, the fluorescence dynamic is explained by the release of the fluorophores by intact granules. The released green fluorophores increased in fluorescence in the more basic cytosol.

Regardless of the potential mechanisms, it is also unclear what caused gut granule flashing to occur. Flashing could either be caused by stimulation via blue light or could occur spontaneously under normal physiological conditions. We reasoned the former to

be more likely, as the phenomenon was usually not observed immediately upon illumination. However, we do not rule out the possibility that gut granule flashing is naturally occurring. In the *ex-vivo* setting, the phenomena were highly associated with the immediate presence of food (Figure 3), which may suggest that the phenomena could be a part of or a consequence of a metabolic or signaling process in food intake. One possibility is that this phenomenon is associated with a vesicle content release of the gut granules, and the fluorophores or the content released play metabolic or signaling roles in food uptake.

Further understanding of gut granule flashing may require the characterization of the green and red fluorophores. It is unclear how to best identify these fluorophores, although we would predict that the green fluorophores emit stronger fluorescence under high pH conditions, while the red fluorophores are likely pH neutral. The visually spectacular fluorescence dynamics may provide assays for biogenesis and function of these lysosome-related organelle.

Data Availability Statement

Strains are available upon request. Supplemental files available at FigShare.

Acknowledgments

We thank members of the Sternberg and Anderson laboratories for experimental support and discussions, particularly David J. Anderson, Han Wang, Xuan Wan, and Stephanie Nava, for their involvement in the earlier stages of this research. We would especially like

to thank David J. Anderson and Hillel Schwartz for their valuable suggestions and critical reading of the manuscript. The five times out-crossed *glo-1(zu391 lf)* X (Hermann et al., 2005) mutant strain OJ1347 (Wang et al., 2013) was a gift from Derek Sieburth of the University of Southern California. This work was also facilitated by WormBase, a knowledgebase for nematode research (Davis et al. 2022). This research was funded by NIH award UF1NS111697 to PWS.

Materials and Methods

Nematode strains maintenance and general methods.

The culture and maintenance of *C. elegans* were done similarly to standard procedures as described in Brenner (1974). Briefly, worms were cultured on 6cm Petri dishes containing Nematode Growth Medium (NGM) agar a bacterial lawn of *Escherichia coli* strain OP50 at 20°C. The Bristol N2 strain (Brenner 1974) was used as the wild-type reference strain and is the strain from which the *glo-1* mutant strain was derived. The five times out-crossed *glo-1(zu391*lf*)* X (Hermann et al. 2005) mutant strain OJ1347 (Wang et al. 2013) was a gift from Dr. Derek Sieburth of the University of Southern California. The culture and maintenance of *S. hermaphroditum* were done similarly standard procedures described in Cao et al. (2022) with minor modifications. Briefly, worms were cultured on 10cm Petri dishes containing Nematode Growth Medium (NGM) agar with a bacterial lawn of *Xenorhabdus griffiniae* strain HGB2511 at 25°C. *X. griffiniae* was cultured in LB medium at 30°C before seeding the lawn.

Preparation of *C. elegans* dauer larvae

To induce dauers, 10-20 young adults were placed on 35 mm diameter Petri dishes containing 2 mL of NGM agar (without peptone) supplemented with a quantity of crude pheromone extract (Schroeder and Flatt 2014) that normally induced 95-100% of dauers

in wild-type animals – typically 10-30 µL per 2 mL of agar. Plates were seeded with 10 µL of 8% w/v *E. coli* OP50 that had been heat-killed at 95°C for 5 minutes. Adults were picked onto the plate and allowed to lay eggs at room temperature (RT; 22-23°C) for 5-9 hours before being removed, during which time they typically laid 200-300 eggs. The plates were then further seeded with an additional 20-50 µL of heat-killed OP50. Afterwards, the plates were wrapped with Parafilm and incubated at 25.5°C for 60-72 hours. Dauers were then picked from this plate for imaging.

in-vivo imaging and analysis of gut granule autofluorescence dynamics

in-vivo imaging and analysis was performed with a Zeiss Imager Z2 microscope equipped with an Apotome 2 and Axiocam 506 mono using Zen 2 Blue software. Worms were partially immobilized with 1mM levamisole in S-basal medium (Stiernagle 2006) and mounted on 5% agarose pads on microscope slides and observed with 100X objective. The excitation wavelength (filter) was 450-490nm, and the emission filter was 500-550nm. If no “flashing” dynamic (as described above) was observed after 230-300s of continuous imaging (as described below) the worm was characterized as not flashing. Image series (or video) were acquired at a rate of about 5 frames per second except for the experiments with L4 stage *C. elegans* larvae, which were acquired at a rate of about 6.5 frames per second.

Sample preparation for _ex-vivo_ imaging.

L4 stage hermaphrodite worms were transferred to a drop of Iwasaki–Teramoto (I–T) solution (Teramoto and Iwasaki 2006) [136mM NaCl, 9mM KCl, 1mM $CaCl_2$, 3mM $MgCl_2$, 77mM D-glucose, and 5mM HEPES (pH 7.4)] and immobilized with 1mM levamisole on a microscopic slide. To expose the intestine for imaging, worms were incised with a pair of 30G 5/8” needles (PrecisionGlide, BD, Franklin Lakes, NJ) near the anus. For experiments with food added on the slide, a glob of OP50 collected by scraping the lawn off an NGM plate using a cell scraper was transferred into the droplet using a

platinum-wire worm pick. A circle was drawn using a PAP pen (RPI) around the solution droplet to avoid spilling, and a piece of cover glass was subsequently mounted on top.

Confocal Microscopy

Confocal time series were acquired using a Fluoview FV3000 Confocal laser scanning biological microscope with a 60×, 1.30 N.A. silicone oil objective (Olympus). Frame rate was calibrated to 1Hz by adjusting the size of the imaging window and the line averaging multiplier. Five minutes of time lapse images were acquired for each sample. All image processing and analyses were done using ImageJ (National Institutes of Health). The transmitted light channel was illuminated simultaneously with the imaging laser (473nm) for positional imaging. Panel A1 in Figures 4, as well as Panels B2, D2, F2 and G in Figure 3, were pseudo-colored with mpl-inferno LUT in FIJI (Schindelin et al. 2012).

Confocal Imaging data processing

ROIs of granules were manually selected in FIJI for all data. For Figure 2(G-H), ROIs of peri-granule “cloud” were defined based on the identification of fluorescent pattern of flashing events, as the surrounding rings that do not overlap with the granule. The zero points of the time series data were set at the flashing onsets of each granule and pooled into metadata.

ROI selection: ROIs were defined based on visual identification of granules in the intestine region, fluorescence normalization baseline was set accordingly as the average of the period prior to the changes in fluorescence. Standard deviation envelopes were visualized in the time series. For Figure 3(H), the number of gut granule flashing events was normalized as per minute $*10^4$ μm^2 of the intestinal surface area from single optical sections, which are manually delineated (Figure 3(G)). Nonparametric Mann-Whitney U test was used for comparison between WT (wild-type) food vs. no-food, and WT food vs. *glo-1(*lf*)*.

Light Stimulus and Locomotion Analysis

Locomotion analysis and animal size measurement were done similarly to what was described in Tan et al. (2022) and Wong et al. (2019) with adaptations. Briefly, at least an hour before the experiment, young adult worms (1 day post-L4) were transferred to NGM plates freshly seeded with 50µl of OP50. Five worms were transferred per plate. The recording and tracking of the worms were performed using WormLab (MBF Bioscience, Williston, VT) equipment and software. The camera was a Nikon AF Micro 60/2.8D with zoom magnification. Each plate was recorded for 2 minutes without stimulus followed by 5 minutes of blue light stimulus. The raw data from the WormLab was then manually processed by matching the tracking data with the recorded video. The average speed shown in Figure 5 was based on the average of the absolute value of the locomotion data (recorded at the frequency of 7.5Hz) collected at the time span of 2 seconds (15 frames).

Data and statistical analysis

Data were plotted as mean ± s.d, except in Figure 3(H), as raw data failed to passed all normality tests (Kolmogorov-Smirnov test, Shapiro-Wilk test, D'Agostino & Pearson test). Data in Figure 3(H) were plotted as median ± 95% CI instead. Student's *t*-test was used in Figure S1.

References

Babu, P., 1974 Biochemical Genetics of Coenorhabditis-Elegans. *Molecular and General Genetics* 135 (1):39-44.

Bhatla, N., and H.R. Horvitz, 2015 Light and hydrogen peroxide inhibit C. elegans Feeding through gustatory receptor orthologs and pharyngeal neurons. *Neuron* 85 (4):804-818.

Brenner, S., 1974 The genetics of Caenorhabditis elegans. *Genetics* 77 (1):71-94.

Cao, M., H.T. Schwartz, C.H. Tan, and P.W. Sternberg, 2022 The entomopathogenic nematode Steinernema hermaphroditum is a self-fertilizing hermaphrodite and a genetically tractable system for the study of parasitic and mutualistic symbiosis. *Genetics* 220 (1).

Chitwood, B., and M. Chitwood, 1950 Introduction to nematology (reprinted 1974). Baltimore: University Park Press.

Chun, H., A.K. Sharma, J. Lee, J. Chan, S. Jia *et al.*, 2017 The Intestinal Copper Exporter CUA-1 Is Required for Systemic Copper Homeostasis in Caenorhabditis elegans. *Journal of Biological Chemistry* 292 (1):1-14.

Clokey, G.V., and L.A. Jacobson, 1986 The autofluorescent "lipofuscin granules" in the intestinal cells of Caenorhabditis elegans are secondary lysosomes. *Mech Ageing Dev* 35 (1):79-94.

Cobb, N.A., 1914 Rhabditin: contribution to a science of nematology. *The Journal of Parasitology* 1 (1):40-41.

Coburn, C., E. Allman, P. Mahanti, A. Benedetto, F. Cabreiro *et al.*, 2013 Anthranilate fluorescence marks a calcium-propagated necrotic wave that promotes organismal death in C. elegans. *PLoS Biol* 11 (7):e1001613.

Dal Santo, P., M.A. Logan, A.D. Chisholm, and E.M. Jorgensen, 1999 The inositol trisphosphate receptor regulates a 50-second behavioral rhythm in C. elegans. *Cell* 98 (6):757-767.

Davis, B.O., Jr., G.L. Anderson, and D.B. Dusenbery, 1982 Total luminescence spectroscopy of fluorescence changes during aging in Caenorhabditis elegans. *Biochemistry* 21 (17):4089-4095.

Davis, P., M. Zarowiecki, V. Arnaboldi, A. Becerra, S. Cain *et al.*, 2022 WormBase in 2022-data, processes, and tools for analyzing Caenorhabditis elegans. *Genetics*.

Delevoye, C., M.S. Marks, and G. Raposo, 2019 Lysosome-related organelles as functional adaptations of the endolysosomal system. *Curr Opin Cell Biol* 59:147-158.

Edwards, S.L., N.K. Charlie, M.C. Milfort, B.S. Brown, C.N. Gravlin *et al.*, 2008 A novel molecular solution for ultraviolet light detection in Caenorhabditis elegans. *PLoS Biol* 6 (8):e198.

Forge, T.A., and A.E. Macguidwin, 1989 Nematode autofluorescence and its use as an indicator of viability. *J Nematol* 21 (3):399-403.

Hajdu, G., M. Somogyvari, P. Csermely, and C. Soti, 2023 Lysosome-related organelles promote stress and immune responses in C. elegans. *Commun Biol* 6 (1):936.

Hedrick, L.R., 1935 *Taxonomy of the nematode genus Spiroxys (family Spiruridae) ... The life history and morphology of Spiroxys contortus (Rudolphi); Nematoda: Spiruruidae*. Ann Arbor? Mich.,.

Hermann, G.J., L.K. Schroeder, C.A. Hieb, A.M. Kershner, B.M. Rabbitts *et al.*, 2005 Genetic analysis of lysosomal trafficking in Caenorhabditis elegans. *Mol Biol Cell* 16 (7):3273-3288.

Klass, M.R., 1977 Aging in the nematode Caenorhabditis elegans: major biological and environmental factors influencing life span. *Mech Ageing Dev* 6 (6):413-429.

Kostich, M., A. Fire, and D.M. Fambrough, 2000 Identification and molecular-genetic characterization of a LAMP/CD68-like protein from Caenorhabditis elegans. *J Cell Sci* 113 (Pt 14):2595-2606.

Laufer, J.S., P. Bazzicalupo, and W.B. Wood, 1980 Segregation of developmental potential in early embryos of Caenorhabditis elegans. *Cell* 19 (3):569-577.

Le, H.H., C.J. Wrobel, S.M. Cohen, J. Yu, H. Park *et al.*, 2020 Modular metabolite assembly in Caenorhabditis elegans depends on carboxylesterases and formation of lysosome-related organelles. *Elife* 9.

Lee, H.J., W. Zhang, D. Zhang, Y. Yang, B. Liu *et al.*, 2015 Assessing cholesterol storage in live cells and C. elegans by stimulated Raman scattering imaging of phenyl-Diyne cholesterol. *Sci Rep* 5:7930.

Luke, C.J., S.C. Pak, Y.S. Askew, T.L. Naviglia, D.J. Askew *et al.*, 2007 An intracellular serpin regulates necrosis by inhibiting the induction and sequelae of lysosomal injury. *Cell* 130 (6):1108-1119.
Maupas, E., 1900 *Modes et formes de reproduction des nematodes*.
Morris, C., O.K. Foster, S. Handa, K. Peloza, L. Voss *et al.*, 2018 Function and regulation of the Caenorhabditis elegans Rab32 family member GLO-1 in lysosome-related organelle biogenesis. *PLoS Genet* 14 (11):e1007772.
Pincus, Z., T.C. Mazer, and F.J. Slack, 2016 Autofluorescence as a measure of senescence in C. elegans: look to red, not blue or green. *Aging (Albany NY)* 8 (5):889-898.
Roh, H.C., S. Collier, J. Guthrie, J.D. Robertson, and K. Kornfeld, 2012 Lysosome-related organelles in intestinal cells are a zinc storage site in C. elegans. *Cell Metab* 15 (1):88-99.
Schindelin, J., I. Arganda-Carreras, E. Frise, V. Kaynig, M. Longair *et al.*, 2012 Fiji: an open-source platform for biological-image analysis. *Nat Methods* 9 (7):676-682.
Schroeder, L.K., S. Kremer, M.J. Kramer, E. Currie, E. Kwan *et al.*, 2007 Function of the Caenorhabditis elegans ABC transporter PGP-2 in the biogenesis of a lysosome-related fat storage organelle. *Mol Biol Cell* 18 (3):995-1008.
Schroeder, N.E., and K.M. Flatt, 2014 In vivo imaging of Dauer-specific neuronal remodeling in C. elegans. *J Vis Exp* (91):e51834.
Stiernagle, T., 2006 Maintenance of C. elegans. *WormBook*:1-11.
Sun, F., Z. Zhao, M.M. Willoughby, S. Shen, Y. Zhou *et al.*, 2022 HRG-9 homologues regulate haem trafficking from haem-enriched compartments. *Nature* 610 (7933):768-774.
Tan, C.H., H. Park, and P.W. Sternberg, 2022 Loss of famh-136/ FAM136A results in minor locomotion and behavioral changes in Caenorhabditis elegans. *MicroPubl Biol* 2022.
Teramoto, T., and K. Iwasaki, 2006 Intestinal calcium waves coordinate a behavioral motor program in C. elegans. *Cell Calcium* 40 (3):319-327.
Thomas, J.H., 1990 Genetic analysis of defecation in Caenorhabditis elegans. *Genetics* 124 (4):855-872.
Thomas, L.J., and H. Quastler, 1950 Preliminary report of X-ray effects on the nematode Rhabditis strongyloides. *Science* 112 (2909):356-357.
Wang, H., K. Girskis, T. Janssen, J.P. Chan, K. Dasgupta *et al.*, 2013 Neuropeptide secreted from a pacemaker activates neurons to control a rhythmic behavior. *Curr Biol* 23 (9):746-754.
Ward, A., J. Liu, Z. Feng, and X.Z. Xu, 2008 Light-sensitive neurons and channels mediate phototaxis in C. elegans. *Nat Neurosci* 11 (8):916-922.
Wong, W.R., K.I. Brugman, S. Maher, J.Y. Oh, K. Howe *et al.*, 2019 Autism-associated missense genetic variants impact locomotion and neurodevelopment in Caenorhabditis elegans. *Hum Mol Genet* 28 (13):2271-2281.

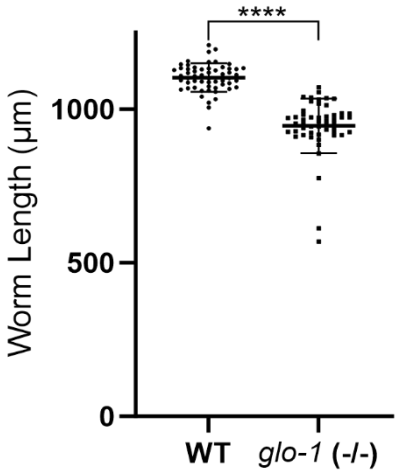

Figure S1 *glo-1(zu391)* worms are slightly smaller compared to the wild type. Values are mean and error bars indicate Standard Deviation (WT: n=57; *glo-1(zu391)*: n=52) (****: p<0.0001, Student's *t*-test).

Video S1 Dynamic fluorescent intensities change in intestinal granules of a dauer stage *C. elegans* larva. Snapshots of this video are shown in Figure 1. Gut granule flashing can be seen starting at about 0:00:20 in this video.

Video S2 Dynamic fluorescent intensities change in intestinal granules of an L4 stage *C. elegans*. Snapshots of this video are shown in Figure 1. Gut granule flashing can be seen starting at about 0:01:20 in this video.

Video S3 Dynamic fluorescent intensities change in intestinal granules of an L4 stage *C. elegans*. The video was taken with a scanning confocal microscope in the *ex-vivo* setting.

Video S4 Dynamic fluorescent intensities change in intestinal granules of an J1 stage *S. hermaphroditum*. Snapshots of this video are shown in Figure 6. Gut granule flashing can be seen starting at about 0:00:30 in this video.